Suppression of Tumorigenicity in Breast Cancer Cells by the Microfilament Protein Profilin 1

By Jürgen Janke,* Kathrin Schlüter,‡ Burkhard Jandrig,*
Michael Theile,* Konrad Kölble,§¶ Wolfgang Arnold,‖
Edgar Grinstein,* Arnfried Schwartz,* Lope Estevéz-Schwarz,¶
Peter M. Schlag,¶ Brigitte M. Jockusch,‡ and Siegfried Scherneck*

From the *Department of Medical Genetics, Max-Delbrück-Center for Molecular Medicine, 13092
Berlin-Buch, Germany; the* ‡*Department of Cell Biology, Zoological Institute, Technical University of
Braunschweig, 38106 Braunschweig, Germany; the* §*Institute of Pathology, Charité Hospital,
Humboldt University, 10117 Berlin, Germany;* ‖*HepaVec GmbH, 13125 Berlin-Buch, Germany;
and the* ¶*Clinic of Surgery and Surgical Oncology, Robert Roessle Hospital, 13122 Berlin-Buch,
Germany*

Abstract

Differential display screening was used to reveal differential gene expression between the tumorigenic breast cancer cell line CAL51 and nontumorigenic microcell hybrids obtained after transfer of human chromosome 17 into CAL51. The human profilin 1 (PFN1) gene was found overexpressed in the microcell hybrid clones compared with the parental line, which displayed a low profilin 1 level. A comparison between several different tumorigenic breast cancer cell lines with nontumorigenic lines showed consistently lower profilin 1 levels in the tumor cells. Transfection of PFN1 cDNA into CAL51 cells raised the profilin 1 level, had a prominent effect on cell growth, cytoskeletal organization and spreading, and suppressed tumorigenicity of the stable, PFN1-overexpressing cell clones in nude mice. Immunohistochemical analysis revealed intermediate and low levels of profilin 1 in different human breast cancers. These results suggest profilin 1 as a suppressor of the tumorigenic phenotype of breast cancer cells.

Key words: tumor suppressor genes • microcell hybrids • cytoskeleton • actin filament • differential display

Introduction

Previously, we established an experimental system consisting of a tumorigenic breast cancer cell line, CAL51, derived from an invasive adenocarcinoma (1), and several nontumorigenic CAL51 microcell hybrid clones obtained after transfer of parts of the human chromosome 17 (2). We focused on hybrid clone CAL/17-5 containing a transferred chromosome region 17p13.3 and distal parts of this chromosome, showing a strongly suppressed neoplastic phenotype with a clearly reduced growth rate and alterations in cell morphology compared with CAL51 (2).

The significance of the 17p13.3 chromosome region for tumorigenicity has been demonstrated by the identification of a candidate tumor suppressor gene, HIC-1 (3), and the discovery of two candidate tumor suppressor genes in ovarian carcinoma (4) in this region. In addition, reports on loss of heterozygosity suggest the involvement of at least one further tumor suppressor gene in the 17p13.3 region (5). Taken together, this information prompted us to evaluate, by differential display (6), altered expression of genes in our experimental systems.

Here, we show that the human profilin 1 (PFN1)[1] gene is expressed at a high level in the microcell hybrid clone CAL/17-5 and at a much lower level in the breast cancer cell line CAL51. The chromosomal localization of PFN1 at 17p13.3 (7) is consistent with the chromosomal fragment transferred into the CAL51 microcell hybrid clones (2). Profilins are small (14–17 kD) ubiquitous proteins that are important regulators of F-actin dynamics in cells (8, 9). Profilins bind monomeric actin (G-actin) and, depending on the conditions, may either inhibit or promote actin fila-

Address correspondence to Siegfried Scherneck, Max-Delbrück-Center for Molecular Medicine, Robert-Rössle-Str. 10, 13092 Berlin, Germany. Phone: 49-30-9406-2226; Fax: 49-30-9406-3842; E-mail: sschern@mdc-berlin.de

[1]*Abbreviations used in this paper:* DTT, dithiothreitol; FBS, fetal bovine serum; PBGD, porphobilinogen deaminase/hydroxymethylbilane synthase; PFN1, profilin 1 gene; RT, reverse transcription.

ment assembly (10–12). In addition, they bind phospholipids (13, 14) and polyproline motif proteins like formins (15) and members of the Enabled (Ena)/mammalian Enabled (Mena)/vasodilator-stimulated phosphoprotein (VASP) family (16), thus being linked to several signal transduction pathways. The precise role of profilin in vivo is still under debate. To correlate the effects of changes in PFN1 expression with the specific properties of CAL51, we transfected human PFN1 cDNA into CAL51 cells and isolated derivative clones expressing different profilin 1 levels. We show that the sole expression of exogenous PFN1 affects growth, cytoskeletal organization, cell spreading, and tumorigenicity of CAL51 cells when injected into nude mice. Furthermore, we demonstrate that the profilin 1 level in several other tumorigenic and nontumorigenic breast epithelial lines and breast cancer tissue, respectively, correlates with their transformed state, suggesting a general role for profilin 1 as a tumor suppressor protein.

Materials and Methods

Cell Culture. The cell line CAL51 (1), its nontumorigenic microcell hybrid CAL/17-5 (2), and the mock-transfected line CALX8, were grown in DMEM supplemented with 10% fetal bovine serum (FBS). For the microcell hybrid and the transfected cells, the medium was supplemented with 800 μg/ml G418. Mouse A9(neo17) cells, containing a single human chromosome 17 derived from normal human fibroblasts and tagged with the neomycin resistance gene (17), were also grown in this medium. MCF-10A, H184, R30, R103, and T47D cells were grown in a 1:1 mixture of DMEM and Ham's F12 medium supplemented with 20 ng/ml epidermal growth factor, 100 ng/ml cholera toxin, 0.01 mg/ml insulin, 500 ng/ml hydrocortisone, and 5% FBS.

RNA Isolation and Differential Display. Total cytoplasmic RNA from CAL51 and CAL/17-5 cells was isolated from $\sim$10^6 cells using a standard protocol (18). 2.0 μg total RNA was used to synthesize first strand cDNAs by Moloney murine leukemia virus reverse transcriptase (GIBCO BRL) using specific 3′ primers dT$_{11}$[A,C,G]N (2.5 μM). Transcription buffer (1×; GIBCO BRL), dithiothreitol (DTT, 10 μM), dNTPs (20 μM), RNasin (10 U), and reverse transcriptase (200 U) were added to 20 μl (final volume). After incubation at 37°C for 1 h, the reaction was terminated by incubation at 95°C for 10 min.

The cDNAs were amplified by PCR, using combinations of the 12 specific 3′ primers and 20 arbitrary 5′ primers according to the manufacturer's instructions (Operon). The PCR reaction mix contained in a final volume of 20 μl: 2 μl first strand cDNA, 3′ primer (2 μM), 5′ primer (0.5 μM), dNTPs (2.0 μM), [α-^{32}P]dCTP (6 μCi), 1× Taq DNA polymerase reaction buffer, and Taq DNA polymerase (1.5 U) (PerkinElmer). Reactions were performed in a PerkinElmer 9600 thermal cycler and consisted of cycles at 95°C for 5 min, followed by 94°C for 30 s, 40°C for 60 s, and 72°C for 30 s for a total of 40 cycles. PCR products from both cell lines were electrophoretically separated on a 6% polyacrylamide gel, vacuum-dried at 80°C for 1 h, and exposed to an x-ray film overnight. Indicated bands were excised from the gel and eluted in 100 μl TE buffer at 4°C overnight. Eluted DNA was reamplified by two successive PCRs using the same conditions as described above. PCR products were run on a 2% agarose gel, visualized by ethidium bromide staining, excised,

and purified using the QIAquick Gel Extraction kit (Qiagen). The purified PCR products were cloned into the pCRII vector, using the TA Cloning kit according to the manufacturer's protocol (Invitrogen).

Northern Blot Analysis. 15 μg of total RNA from CAL51 and CAL/17-5 cells was heat-denatured at 55°C for 15 min, electrophoretically separated on a 1.2% agarose/1.1% formaldehyde gel, and transferred to a Hybond membrane (Amersham Pharmacia Biotech) by vacuum blotting in 20× SSC. The RNA was cross-linked to the membrane by UV fixation (Stratalinker®; Stratagene) for 1 min. A ^{32}P-labeled cDNA probe was generated from the cloned PCR product (80 ng plasmid) by amplification (conditions as described above) in the presence of [α-^{32}P]dCTP (50 μCi). Hybridization and stripping of Northern blots were carried out according to standard procedures (19). After stripping the membranes, a loading control with ^{32}P-labeled β-actin cDNA probe was performed. The blots were exposed to a PhosphorImager® screen and analyzed with ImageQuant® software (Molecular Dynamics).

Reverse Transcription PCR. Total RNA was prepared from cultured cell lines using TRIZOL (Life Technologies) and cDNA synthesized from 1 μg of total RNA. Reverse transcription (RT) was performed in a 20 μl volume of 1× first strand buffer, 10 mM DTT, 500 μM of each dNTP, 200 U of Super-Script II Reverse Transcriptase (all reagents from Life Technologies), 500 ng of oligo-dT, and 20 U of RNasin (Promega). RNA and primer were heated at 70°C for 5 min and immediately chilled on ice before the addition of RNasin, first strand buffer, DTT, dNTPs, and reverse transcriptase. Samples were incubated at 42°C for 30 min, and the reaction was stopped by incubation at 94°C for 5 min.

As endogenous RNA control, we selected the porphobilinogen deaminase/hydroxymethylbilane synthase (PBGD) gene (20) because no corresponding retropseudogenes exist so far in contrast to β-actin, glyceraldehyde 3-phosphate dehydrogenase, and hypoxanthine ribosyltransferase (21). The oligonucleotides used in PCR amplification were as follows: profilin P1 (sense strand in exon 1), 5′-CGAGAGCAGCCCCAGTAGCAGC-3′; profilin P2 (antisense strand in exon 2), 5′-ACCAGGACAC-CCACCTCAGCTG-3′, resulting in a 179-bp PCR product; and PBGD-S (sense strand in exon 1), 5′-TGTCTGGTAACG-GCAATGCGGCTGCAAC-3′, resulting in a 126-bp PCR product. PCR was performed in a 20-μl volume of 1× PCR buffer, 200 μM of each dNTP, 1.5 U Taq DNA polymerase (all reagents from PerkinElmer), and 0.5 μM of primers with 2 μl cDNA. PCR consisted of an initial denaturation step at 95°C for 3 min, followed by 30 cycles at 95°C for 20 s, annealing at 60°C for 15 s, and extension at 72°C for 30 s in each cycle using a GeneAmp PCR System 9600 (PerkinElmer). PCR products were separated on 3:1 NuSieve agarose gels (FMC Bioproducts) and visualized by ethidium bromide staining. The ImageQuant® Software was used for analysis.

Sequence Analysis. The cloned PCR fragments were sequenced using an ABI DNA sequencer, T7 or M13 reverse primer, and the Dye Terminator Cycle Sequencing kit according to the manufacturer's protocol (PE Biosystems). A minimum of two independent clones of each PCR fragment was sequenced to exclude that different PCR products with the same length were excised from the polyacrylamide gel. The cDNA sequences were compared with sequences in the EMBL/GenBank/DDBJ database, using FASTA and BLASTN.

Preparation of Cell Lysates and Western Blot Analysis. Cell lysates were prepared as described (22). SDS-PAGE and Western

immunoblot analysis were performed according to standard procedures. The monoclonal profilin 1 antibody, 2H11 (23), was used at a 1:10 dilution, and an mAb against β-actin (Sigma-Aldrich) was used at a 1:2,000 dilution. After incubation with peroxidase-conjugated anti–mouse IgG antibody (1:10,000 dilution; Promega), immunoreactive bands were detected by the enhanced chemiluminescence method (Amersham Pharmacia Biotech). For quantitation of profilin 1 content, the gel evaluation system E.A.S.Y. (Herolab) was used. For CAL51 and its derivatives, profilin 1 was expressed as relative value normalized to the β-actin content. For the comparison between the tumorigenic breast cancer lines and their normal counterparts, profilin 1 was expressed as absolute value per standard amount of total protein. Regression constants obtained with standard profilin 1 curves were in the range of 0.97–0.99.

Immunofluorescence Analysis. Cells were grown on glass coverslips for 24 h before fixation in 4% formaldehyde for 20 min, and subsequent extraction with 0.2% Triton X-100 for 10 min. Next, the samples were incubated for 1 h at room temperature in a moist chamber with 2H11 (23). Goat anti–mouse IgG coupled to tetramethylrhodamine-B-isothiocyanate (TRITC; Dianova) was used as secondary antibody and phalloidin-FITC for labeling of F-actin. The cells were examined with a conventional light microscope equipped with epifluorescence (Axiophot; ZEISS). All photographs were taken with the same exposure time.

cDNA Cloning. PFN1 cDNA was amplified from a CAL/17-5 cDNA library by PCR using PFN1-specific primers 5′-GAG-GCAGCTCGAGCCCAGTC-3′ and 5′-AAATGGTTTGT-GTGTGTATG-3′ (sequence data available from EMBL/Gen-Bank/DDBJ under accession no. J03191, and see reference 7). The cycling parameters were as follows: 95°C for 5 min, followed by 94°C for 30 s, 60°C for 30 s, and 72°C for 45 s for a total of 35 cycles and an extension at 72°C for 10 min. The purified 546-bp fragment was cloned into the pCRII vector, excised with EcoRI, and recloned into the eukaryotic expression vector pcDNA3 (Invitrogen), which contains the neo^R gene as a selection marker, resulting in the plasmid pcDNA3-P. Orientation and integrity of the vector construct were confirmed by sequencing in both orientations.

Transfection of CAL51 Cells with PFN1 cDNA. Purified plasmid DNAs (pcDNA3-P and pcDNA3; 2 μg in each case) were transfected into CAL51 cells using 60 μg Lipofectin according to the manufacturer's instructions (Life Technologies). Selection with 800 μg/ml G418 started 48 h after transfection. After 2–3 wk, G418-resistant clones were picked and further propagated in the selective medium. Expression analysis of several clones was performed by RT-PCR. RNA isolation and conditions for RT using an oligo-dT$_{17}$ primer were as above. PCR was carried out as described above, but 2.0 μl first strand cDNA was used as template, and β-actin–specific primers (0.5 μM) were used additionally (duplex PCR). Only 20 cycles were performed. PCR products were separated on a 2% agarose gel, visualized by ethidium bromide staining, and evaluated by using the ImageQuant® software.

In Vitro Growth Assays. Cell growth rates on plastics and colony-forming ability in soft agar were determined as described previously (2). For the extracellular matrix assay, cells were suspended and adjusted to 8.4×10^5 cells per ml culture medium. Then, samples of 60 μl cells were mixed gently with 300 μl Matrigel (Collaborative Biomed, Inc.) at 4°C and plated on 24-well plates. Mixtures were overlaid after gelling with 0.7 ml culture medium containing 2% FBS. Cultures were kept at 37°C in a humidified atmosphere containing 5% CO_2.

The matrigel cultures were fixed in phosphate-buffered 2% paraformaldehyde/12.5% glutaraldehyde in 0.09 M sucrose overnight, cooled for 5 min in isopentane ($-35°C$), and stored at $-80°C$. After a short postfixing in 5% buffered formalin, the cultures were treated in the conventional manner for embedding in paraffin, cut in 5-μm slices, and stained with hematoxylin and eosin.

Cell Spreading. Spreading of CAL51, microcell hybrids, PFN1-transfected CAL51 clones, and MCF-10A was monitored by seeding the cells onto glass coverslips. They were allowed to adhere for 30 min before fixation and processing for fluorescence microscopy. According to their distinct differences in surface area and morphology, the cells were divided into two groups: small, round cells showing no obvious sign of spreading (group 1), and flat cells in the process of spreading or already well spread (group 2). Monitoring the proportion of group 1 to group 2 cells in a given time point after seeding serves as a measure of their spreading velocity. At least 500 cells per coverslip were counted in 4 independent experiments.

Tumorigenicity Test. Suspensions of 10^6 and 10^5 cells, respectively, in a volume of 0.2 ml of serum-free culture medium were injected subcutaneously into 5–8-wk-old female immune-deficient nude mice (BlnA:NMRI-nu/nu). Tumor volumes were estimated as described previously (24). Cell populations were considered to be nontumorigenic if no tumors were detected after 3 mo postinjection.

Immunohistochemical Analysis. Formalin-fixed, paraffin-embedded tissue blocks of 40 cases of invasive breast cancer were retrieved from pathology archives. Immunostaining was performed essentially as described (25). In short, 3-μm sections were subjected to heat-induced antigen retrieval and subsequently incubated with purified mouse mAb 2H11. Antigen–antibody complexes were visualized using biotinylated anti–mouse Ig, streptavidin–alkaline phosphatase conjugate (Jackson ImmunoResearch Laboratories), and Fast Red chromogenic substrate (Sigma-Aldrich). Cellular distribution and intensity of PFN1 expression were scored in comparison with nonneoplastic mammary epithelia and/or leukocytes in the same section.

DNA Isolation and Mutation Analysis. DNA was isolated from washed trypsinized cells or from blood as control using the QIAamp tissue and blood kits (Qiagen). PCR products covering exons 1–3, flanking intronic sequences, and the 5′ end of the PFN1 gene were sequenced with the DyeDeoxy Terminator Cycle Sequencing kit (PE Biosystems) in both directions and run onto an ABI 377 automatic sequencer.

Results

CAL51 Cells Express Low Levels of PFN1 mRNA and Protein, and Show a Low Degree of Microfilament Organization. To monitor possible differences in mRNA levels between tumorigenic CAL51 breast cancer cells and cells from a matched nontumorigenic CAL/17-5 microcell hybrid clone, differential display was performed in duplicate on total RNA from both cell lines. A representative gel using a single primer set is shown in Fig. 1. Several mRNAs were reproducibly differentially expressed. A series of 164 partial cDNAs that displayed a significantly high ratio of differential expression was selected. To date, 40 have been used as probes in Northern blot analysis. For 12 of the 40 cDNAs analyzed, the results of the differential display experiments

A

Differential display
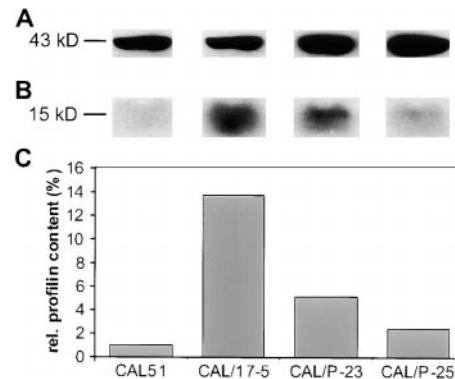

B

Northern blot

C

%
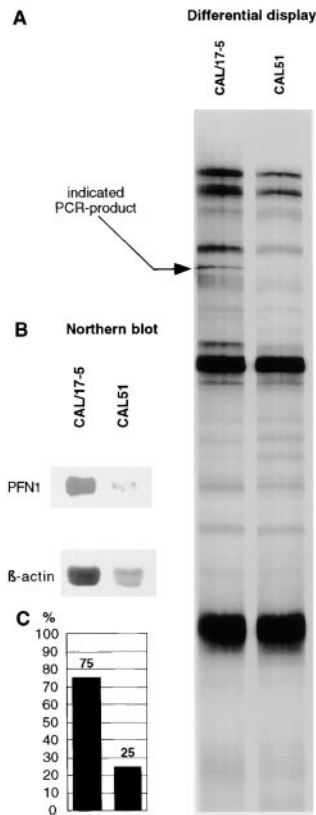
Figure 1. (A) Differential display of the mRNA profiles of CAL51 breast cancer cells versus CAL/17-5 microcell hybrid cells. The indicated RT-PCR product shows a high density band in the CAL/17-5 lane. The PCR product was identified as part of PFN1 cDNA by comparison with database sequences. (B) Northern hybridization of the excised and reamplified PCR fragment confirmed the differential expression. (C) Using a computer program, the PFN1 mRNA values were standardized taking into account the β-actin values. The sum of all PFN1 mRNA values was set to 100. 75% fall on CAL/17-5 and 25% on CAL51.

Figure 2. Western blot analysis of β-actin (A) and profilin 1 (B) in CAL51 (lane 1), the microcell hybrid clone CAL/17-5 (lane 2), the stable PFN1 transfectants CAL/P-23 (lane 3), and CAL/P-25 (lane 4). β-actin and profilin 1 were detected with the respective mAbs. The depicted strips were taken from the same gel. The relative (rel.) profilin 1 content is the ratio of the amount of profilin 1 in CAL51 microcell hybrids and transfectants, respectively, to the profilin 1 amount in CAL51 cells, normalized to the β-actin band and evaluated by a blot evaluation program (C).

were corroborated by this method. Some of these cDNAs displayed important homology with previously cloned human genes (e.g., Sp17 gene, apolipoprotein J gene; our unpublished data). One of these genes reproducibly exhibited a strongly reduced transcription in CAL51 cells compared with the CAL/17-5 hybrid cells. A FASTA search for sequence homology revealed 98.8% sequence homology to that of human PFN1. Therefore, these results indicate that CAL51 and its microcell hybrid derivative differ substantially in the expression of PFN1 mRNA.

PFN1 protein expression in CAL51 and microcell hybrid cells was then examined by Western blot and immunocytochemistry using the profilin 1–specific antibody 2H11, which recognizes profilin 1 in a wide variety of mammalian cells (23). The Western blot analysis showed that the profilin 1 level in CAL51 cells is low compared with the microcell hybrid clone CAL/17-5 (Fig. 2 B). When normalized to the β-actin level, an almost 14-fold difference between CAL51 and CAL/17-5 was found (Fig. 2 C).

These results were also reflected in the images obtained for both cell types by immunofluorescence. As demonstrated in Fig. 3, the profilin 1–specific stain was very low in the parental CAL51 cells (Fig. 3, top). In contrast, CAL/17-5 cells displayed a moderate to strong reactivity for profilin 1 (Fig. 3, second from top) visible as a diffuse cytoplasmic stain and a distinct concentration in the nucleus. The strong nuclear profilin 1 signal is seen in many cell types after formaldehyde fixation (23). Similar staining pictures were

also obtained with other microcell hybrid clones (data not shown). Thus, Western blot and immunofluorescence both demonstrated a low abundance of profilin 1 in CAL51, and a much higher level in the microcell hybrid CAL/17-5.

The differences in PFN1 expression seen in immunofluorescence were paralleled by conspicuous differences in the actin filament organization: whereas CAL51 cells displayed thin microfilament bundles and short F-actin aggregates distributed throughout the cytoplasm (Fig. 3, top), CAL/17-5 cells showed bundling of actin filaments into thick stress fibers and/or peripheral belts (Fig. 3, second from top). An organization of the actin filaments in peripheral belts is typical for normal epitheloid cells, as for example the breast epithelial cell line MCF-10A (Fig. 3, bottom; reference 23).

The PFN1 Gene Shows Sequence Variations in CAL51 Cells Compared with A9(neo17) Cells and Lymphocytes. To determine whether the low PFN1 mRNA and protein expression in CAL51 reflects a mutated gene, we screened for mutations within the PFN1 gene in both CAL51 and the microcell donor A9(neo17). The three PFN1 exons, as well as 923 bp from the 5′ genome region, were sequenced. For A9(neo17), no differences in the PFN1 gene were found compared with the sequence present in human lymphocytes. For CAL51, sequence variations were detected in exon 3, in the 3′ untranslated region, and in the 5′ region of the PFN1 gene. The homozygous alteration in exon 3, C334T, did not result in an amino acid substitution. A heterozygous deletion (645delT) in the 3′ untranslated gene region is not expected to have major effects on structure or function of the protein product. In contrast, the homozygous alteration (A-773G) within the 5′ promoter region might result in a different binding behavior of specific transcription factors, and therefore may lead to consequences on protein translation; however, in the present case, this is not proven.
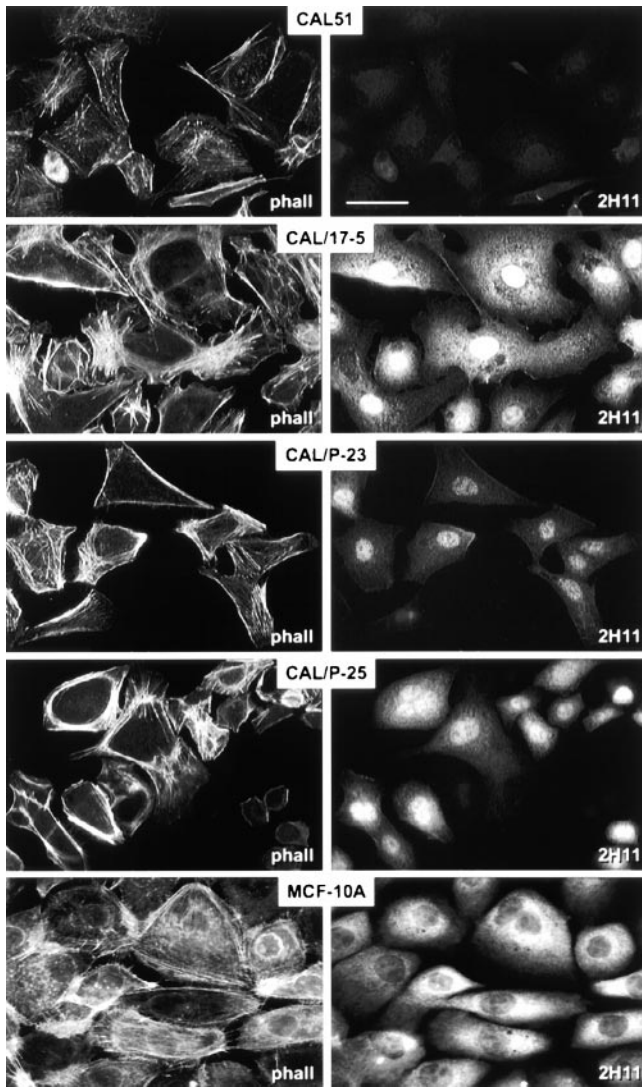
Figure 3. Fluorescence analysis of the actin cytoskeleton of CAL51, CAL/17-5 microcell hybrids, CAL/P-23 and CAL/P-25 PFN1 transfectants, and breast epithelial cells MCF-10A. Cells were double-stained with the profilin 1 mAb 2H11 and TRITC-coupled anti–mouse IgG, and with phalloidin-FITC for F-actin (phall). All pictures were taken with the same exposure times. Bar, 20 μm.

In the microcell hybrid CAL/17-5, both CAL51 and A9(neo17) PFN1 gene sequences were detected (heterozygous for C334T). This finding confirms that the PFN1 gene is indeed present on the transferred chromosome in CAL/17-5.

PFN1 cDNA Transfection into CAL51 Mimics Profilin 1 Level and Distribution In the Microcell Hybrids. To characterize the correlation between profilin 1 levels and the properties of CAL51, CAL51 cells were transfected with the vector pcDNA3-P containing full-length PFN1 cDNA and the neomycin acetyl transferase gene (neo^R) conferring resistance to the aminoglycoside G418. Resistant colonies were selected, and cell clones were isolated and further propagated in medium containing G418. PFN1 expression in the different clones obtained was again examined by Western blot and immunostaining using the antibody 2H11. In two selected clones, CAL/P-23 and CAL/P-25, PFN1 expression was substantially increased (5.1- and 2.4-fold, respectively, normalized to β-actin) compared with CAL51 (Fig. 2). Consistent with the Western blot data, immunofluorescence on cells of these two clones showed moderate to strong profilin 1 staining, and the profilin 1 distribution was similar to that obtained for the microcell hybrid clone CAL/17-5 (Fig. 3). In accordance with the PFN1 expression, the actin filament distribution in CAL/P-23 and CAL/P-25 was similar to that observed for the microcell hybrid clone: the cells displayed well-formed stress fibers and epitheloid peripheral belts (Fig. 3), a morphology also seen in MCF-10A cells (Fig. 3, bottom).

Expression of Exogenous PFN1 Suppresses Transformed and Tumorigenic Properties of CAL51. Previously, we demonstrated that microcell hybrids obtained after transfer of chromosome 17 into CAL51 cells showed a clearly reduced growth rate compared with CAL51 cells (2). In accordance with these results, the PFN1-transfected clones CAL/P-23 and CAL/P-25 showed a marked reduction in growth rate compared with the parental cells and CALX8, a cell line derived from CAL51 cells mock-transfected with the control plasmid pcDNA3 (Fig. 4 A).

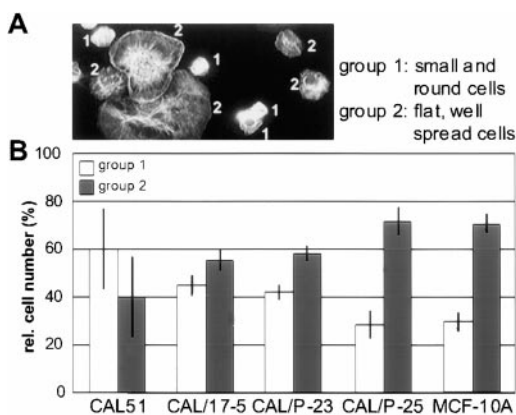Anchorage-independent growth, a generally accepted indicator of the transformed phenotype in vitro (26), was
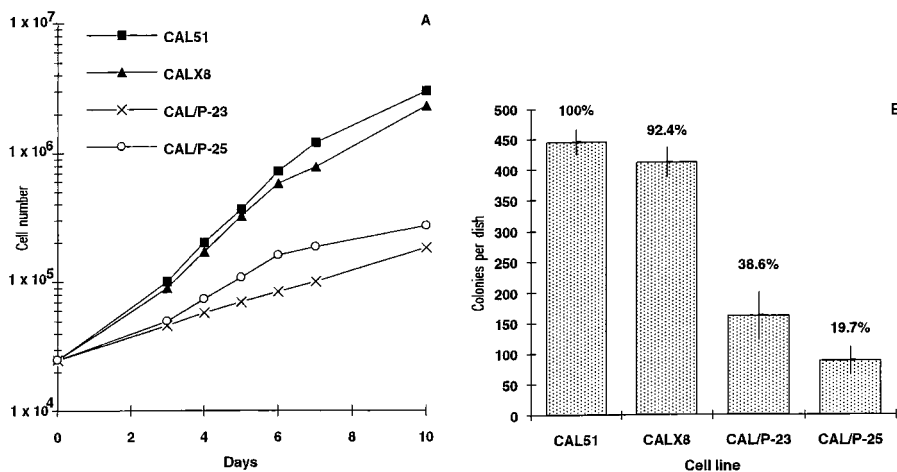
Figure 4. In vitro growth properties of CAL51 and derivatives. (A) Growth curves of CAL51, mock-transfected CAL51 cells (CALX8), and the PFN1-transfected clones CAL/P-23 and CAL/P-25. (B) Growth of the same cell lines in soft agar. 5×10^4 cells were plated per dish. 100% (CAL51) = 4.4 × 10^2 colonies. The data points reflect the means of three independent experiments.

tested by plating the cells in semisolid agar medium. The PFN1-transfected clones CAL/P-23 and CAL/P-25 showed a clearly reduced colony-forming capacity compared with CAL51 and CALX8 cells (Fig. 4 B). In this assay, the level of reduction in the colony-forming ability varied for different transfected clones between 19.7 and 38.6% compared with 100% colony-forming ability for CAL51 cells. There was no partial suppressive effect of the PFN1-transfected clones compared with the CAL/17-5 cells, and growth on plastic and in soft agar was comparable between these cell lines.
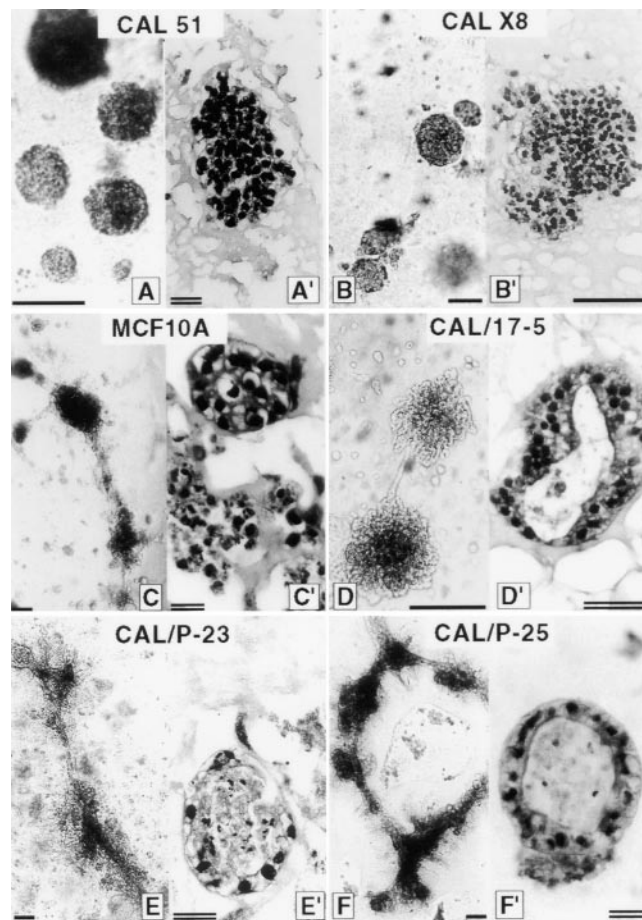
We also found a clear correlation between the profilin 1 content and the spreading behavior of CAL51 and its derivatives. The spreading velocity determines cell contact formation. Thus, in general, normal epithelial cells are expected to spread faster than tumorigenic cells. Inspection of the shape of CAL51, CAL/17-5, CAL/P-23, CAL/P-25, and MCF-10A cells shortly after seeding permitted the assignment of these cells to two distinct categories: round, compact cells and flat, moderately or already well-spread cells (Fig. 5 A). At 30 min after seeding, a high proportion (60%) of the CAL51 cells belonged to the first group, while the majority of the CAL51 derivatives with a higher profilin 1 level were already in group 2 (Fig. 5 B) to the same extent as the normal breast epithelial cell line MCF-10A.

To detect in vivo architectural differences between normal and tumorigenic cells, we used a three-dimensional extracellular matrix assay (27). CAL51 and CALX8 cells, the microcell hybrid CAL/17-5, and the PFN1-transfected clones, CAL/P-23 and CAL/P-25, were plated in Matrigel and compared with respect to their pattern of growth and differentiation to an equal number of MCF-10A cells, a nontransformed breast epithelial line. In each case, initially after plating, the cells were distributed evenly over the sur-

face of the well. After 2–3 wk of incubation in Matrigel cells of the transfected clones, CAL51 cells showed a completely different morphology. The CAL51 cells had formed large colonies with smooth boundaries (Fig. 6 A). A similar result was obtained for the CALX8 control cells (Fig. 6 B). In contrast, the nontransformed breast epithelial cell line MCF-10A formed structures reminiscent of glandular organization. Large, duct-like structures were seen interconnecting multicellular spheres and other aggregates, which displayed fine filamentous, partially branching, projections (Fig. 6 C). Both PFN1-transfected clones, CAL/P-23 and CAL/P-25 (Fig. 6, E and F), as well as the microcell hybrid clone CAL/17-5 (Fig. 6 D), grew in a pattern similar to MCF-10A but distinct from that of CAL51. They also formed structures reminiscent of the mammary alveolar ductal system. Histological sections (Fig. 6, A′–F′) confirmed the alveolar organization: many of these spheres were hollow, and the bordering cells displayed an epithelioid morphology. Such structures were never seen with the CAL51 cells. These data suggest that an elevated profilin 1

Figure 5. Spreading of CAL51, the microcell hybrid CAL17-5, the PFN1 transfectants CAL/P-23 and CAL/P-25, and the breast epithelial cell line MCF10-A. Cells were allowed to adhere to coverslips for 30 min (B), before fixation and phalloidin staining. As seen in A, the cells could be assigned to two groups that differed in the surface area occupied and in their morphology (designated 1 and 2). The proportion of cells in each group was determined. The diagram in B shows the result of 4 independent experiments with at least 500 counted cells per coverslip. Bars indicate SDs.

Figure 6. Growth of CAL51 (A, A′), the mock-transfected control CALX8 (B, B′), the mammary epithelial cell line MCF-10A (C, C′), the microcell hybrid CAL/17-5 (D, D′), and the PFN1 transfectants CAL/P-23 (E, E′) and CAL/P-25 (F, F′) in Matrigel. Total cultures of the different cell types (A–F) and hematoxylin and eosin–stained histological sections (A′–F′) are shown. Bars: (single) 100 μm; (double) 20 μm.

Table I. *Tumorigenicity of CAL51, PFN1-transfected CAL51 Clones, and Microcell Hybrid CAL/17-5 Cells*

Cell line	Inoculated cells per animal	Mice with tumor/ mice injected	Tumor volume (mm³)*									
			1 wk‡	2	3	4	5	6	7	8	9	10
CAL51	10^6	4/4	2	15	144	240	301	368	653	701	846	918
	10^5	4/4	0	1	5	81	90	180	322	404	553	746
CAL/P-23	10^6	1/2	0	0	0	0	0	0	10	32	63	147
	10^5	0/2	0	0	0	0	0	0	0	0	0	0
CAL/P-25	10^6	2/5	0	0	0	0	0	0	25	38	62	62
	10^5	0/3	0	0	0	0	0	0	0	0	0	0
CAL/17-5	10^6	0/3	0	0	0	0	0	0	0	0	0	0
	10^5	0/3	0	0	0	0	0	0	0	0	0	0

*In case of tumor take 4/4: mean values for four animals are represented; tumor take 1/2: value for the animal showing tumor growth is represented; tumor take 2/5: mean values for two animals are represented.
‡Week after injection, 1–10.

level directs the CAL51 cells towards a closer to normal phenotype.

A High Profilin 1 Content Reduces Tumorigenicity of CAL51. The low PFN1 expression in CAL51 breast cancer cells prompted us to examine the consequences of forced expression of PFN1 on the tumorigenic properties of these cells. CAL51 cells, the microcell hybrid clone CAL/17-5, and the PFN1-transfected CAL/P-23 and CAL/P-25 clones were injected subcutaneously into 5–8-wk-old nude mice. Formation of tumors was recorded over a period of >60 d (Table I). CAL51 cells produced progressively growing tumors that were palpable within <1 mo when 10^6 cells were inoculated per animal. In contrast, the clones expressing exogenous PFN1 did not produce palpable tumors even 2 mo after injection, at which time the CAL51-injected animals had all developed tumors. To ensure that the neomycin resistance gene was not responsible for the suppression of the neoplastic phenotype, G418-resistant CALX8 cells were injected into nude mice. These cells were tumorigenic at rates comparable to those of CAL51 (data not shown), indicating that the suppressed phenotypes cannot be attributed to the expression of the neo[R] gene.

Here (Table I), and in earlier experiments (2), we could demonstrate that the tumorigenicity as originally observed in CAL51 cells was completely suppressed when CAL/17-5 and other CAL/17 microcell hybrids were injected into nude mice.

Low Profilin 1 Contents Are Seen In a Variety of Human Breast Cancer Cell Lines and Human Breast Cancer Tissue. Next, we investigated whether the low profilin 1 content of CAL51 cells, as described here, might be a property unique to this particular cell line. By RT-PCR, we analyzed the PFN1 mRNA level of three human breast cancer cell lines in comparison with the two nontumorigenic epithelial cell lines, H184 and MCF-10A, and the CAL/17-5

microcell hybrid, respectively. As seen in Fig. 7, the PFN1 mRNA content of the nontumorigenic cell lines and the CAL/17-5 microcell hybrids showed PFN1 mRNA levels approximately threefold of the values obtained for the tumorigenic lines. Furthermore, by quantitative immunoblots, we analyzed the profilin 1 content of four human breast cancer cell lines in comparison with two nontumorigenic epithelial lines. As seen in Fig. 8 (A and C), the profilin 1 content varied slightly between the tumorigenic lines.
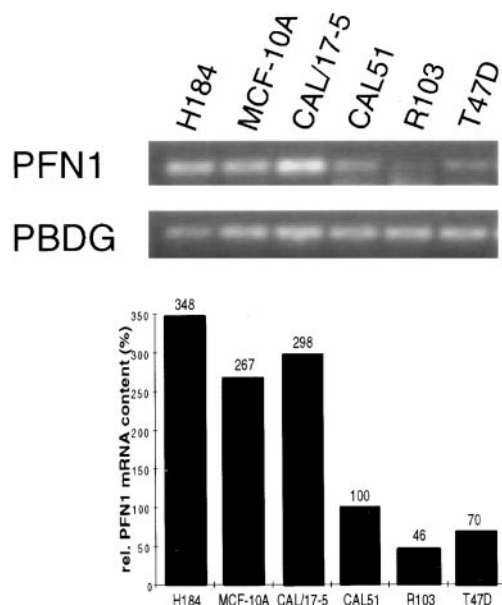

Figure 7. RT-PCR analysis of PFN1 and PBGD expression in H184 (lane 1), MCF-10A (lane 2), CAL/17-5 (lane 3), CAL51 (lane 4), R103 (lane 5), and T47D cells (lane 6). The relative (rel.) PFN1 mRNA content is the ratio of the amount of PFN1 mRNA in the cell lines to the amount in CAL51 cells normalized to the PBGD bands and evaluated by a computer program.
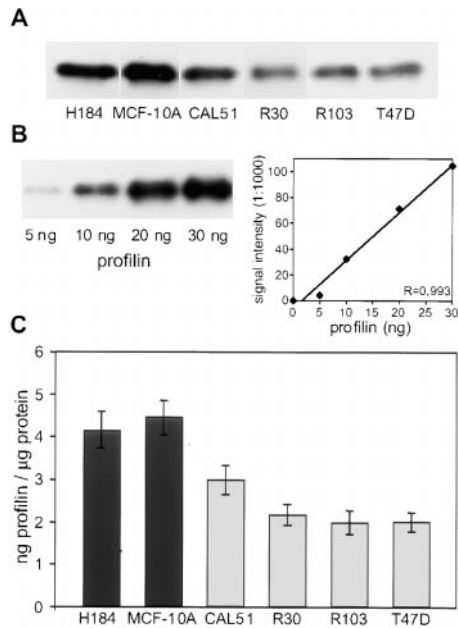
Figure 8. Western blot analysis (A) showing the profilin 1 content in relation to total protein in two normal breast epithelial lines (black bars in C) and four breast cancer lines (gray bars in C). The bars reflect the values from blots obtained with the profilin 1 antibody 2H11, derived from 10 gels containing protein extracts of all 6 lines. SEs are given in C. A representative profilin 1 standard curve is given in B.

Among those, CAL51 did not show an extremely low level. On the other hand, the two nontumorigenic lines investigated, H184 and MCF-10A, showed consistently higher values, with profilin 1 contents ~1.5–2-fold of the values determined for the tumor lines. In contrast, the actin content of tumorigenic and nontumorigenic lines was approximately the same (data not shown). Although preliminary, these data indicate that there may be a consistent difference in profilin 1 levels between tumorigenic and nontumorigenic lines in general, and support the notion that a critical profilin 1 level is required for tumor suppression.

Intermediate and low profilin 1 levels are found in human breast cancer tissue. Immunohistochemically normal lobular and ductal epithelia of the mammary gland show a heterogeneous pattern of PFN1 expression in which individual luminal and basal cells displaying a strong cytoplasmic PFN1 expression are scattered between epithelial cells of intermediate to low levels of expression (Fig. 9 A). This heterogeneity appears greatly reduced in breast cancers where the majority of the invasive cells display a uniform PFN1 expression in their cytoplasm. Compared with nonneoplastic mammary epithelia and/or leukocytes, PFN1 was found to be expressed at intermediate levels (Fig. 9 B) in 31 (78%) and at low levels (Fig. 9 C) in 9 (22%) of the 40 breast cancers studied. Interestingly, one case with intermediate PFN1 expression in the primary tumor showed a low expression in its axillary metastasis (Fig. 9 D).
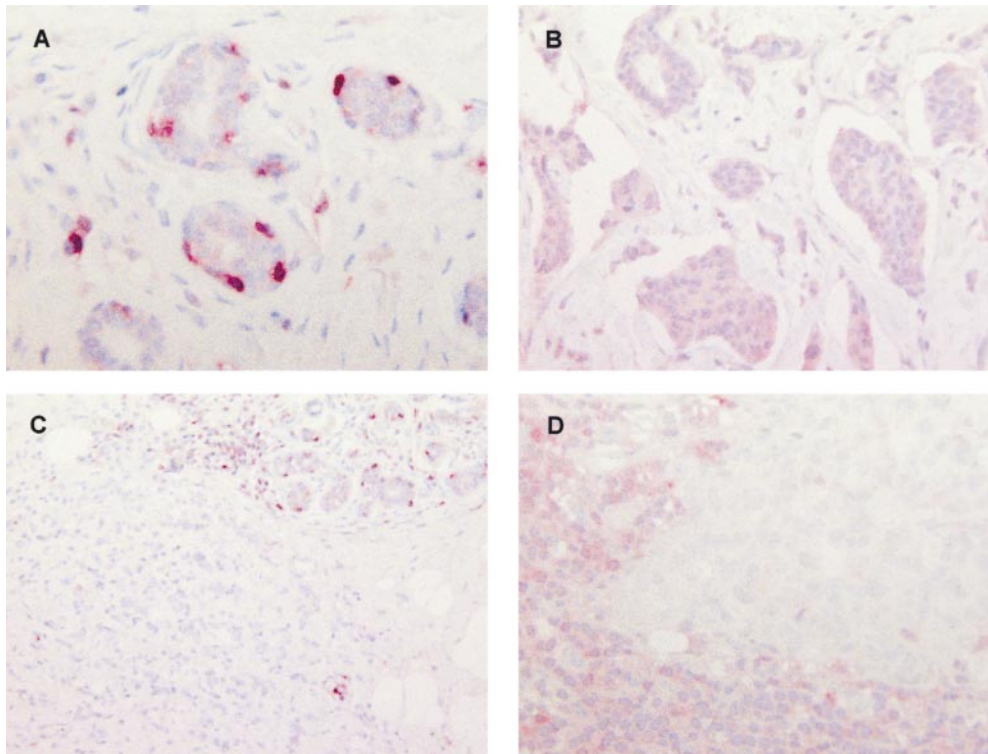
Figure 9. Immunohistochemical expression analysis of PFN1 in human mammary tissues. Paraffin sections were subjected to heat-induced antigen retrieval, and subsequently incubated with purified mouse anti–profilin 1 mAb 2H11. Antigen–antibody complexes were visualized using a biotin/streptavidin–alkaline phosphatase/Fast Red system. (A) Normal breast lobule with heterogeneous intermediate and focally strong expression of PFN1 in the cytoplasm of basal and luminal epithelial cells. (B) Invasive mammary carcinoma with homogenous intermediate expression of PFN1 in the cytoplasm of tumor cells. (C) Formation of invasive mammary carcinoma next to a nonneoplastic lobule. Note the reduced expression of PFN1 in the cancer cells and the retained strong staining of intravascular leukocytes (bottom right). (D) LN metastasis of the primary mammary carcinoma depicted in B with loss of PFN1 expression in the metastatic tumor cells. Residual lymphatic elements retain their pronounced cytoplasmatic expression of PFN1. Original magnifications: (A) ×600; (B) ×400; (C) ×200; and (D) ×600.

Discussion

In this study, differential gene expression was analyzed in an experimental system consisting of a tumorigenic breast cancer cell line, CAL51, and a nontumorigenic CAL/17-5 microcell hybrid, obtained after transfer of human chromosome 17 into CAL51 cells. Differential display was used to identify the pattern of genetic alterations. The PFN1 gene showed a markedly increased expression in the microcell hybrid clone relative to the lower level in CAL51 cells. Differential expression of PFN1 was confirmed by Northern and Western blot analysis, and by immunostaining. The PFN1 gene was mapped to chromosome region 17p13.3 (7), which is the particular part of chromosome 17 identified in the microcell hybrid clones after chromosomal transfer into CAL51 cells (2).

Having identified PFN1 mRNA levels as one of the major differences between CAL51 and its microcell hybrid derivatives, we directly challenged the role of PFN1 expression on the morphological and tumorigenic properties of these breast cancer cells by transfer of PFN1 cDNA. The obtained stable cell lines behaved quite similar to the microcell hybrid clones in the following ways: (a) they showed a higher PFN1 expression, which was correlated with reduced growth rates and a more sophisticated organization of the actin cytoskeleton; (b) they spread much faster on glass, indicating better adhesion properties; (c) they displayed an improved anchorage dependence and the capacity to form epitheloid structures; and (d) they were much less tumorigenic in nude mice. Therefore, the sole elevation of the profilin 1 level drives CAL51 cells towards a more normal epithelial differentiation.

For several tumorigenic and nontumorigenic breast epithelial lines, we found a consistently lower profilin 1 content in the former. These differences did not exceed a factor of three, and more detailed investigations are needed to further substantiate these data. However, they indicate that a critical level of profilin 1 must be exceeded to effect tumor suppression. Similarly low expression of PFN1 is immunohistochemically apparent in >20% of invasive breast cancers. It remains to be seen whether the profilin 1 content reflects stages in tumor progression or marks particular biological and prognostic subsets of mammary carcinoma. On the other hand, a substantial surplus in profilin 1, as found in CAL/17-5 and CAL/P-23, obviously does not interfere with normal cellular functions. An increase in microfilament organization and cell adhesion, as shown here, has also been reported for other cell types overexpressing PFN1 by factors of two to eight (28, 29).

Profilins are ubiquitous, 12–15-kD proteins identified in all eukaryotic systems examined to date, including yeast, amebae, vertebrates, and plants (8, 9, 30). Many organisms contain two genes, PFN1 and PFN2, of which PFN1, widely expressed, is indispensable for normal cellular functions (9). Profilins are thought to regulate signal-dependent actin polymerization (9). The involvement of the actin-based cytoskeleton in many cellular functions, including cell adhesion and motility, growth and cytokinesis, signal transduction, and the establishment and maintenance of cell morphology relies on different states of supramolecular organization, executed by actin-binding proteins (31, 32). Conversely, tumorigenicity, and in particular metastatic capacity, has been frequently correlated with a particular organization of the microfilament system (33, 34). In general, it was assumed that stable microfilament bundles and cell matrix contacts are correlated with normal phenotyes of cells and tissues, while transformation to malignancy, as for example caused by tumor viruses, is accompanied by reduced expression of proteins such as tropomyosin (35), α-actinin (36), and vinculin (37, 38). These proteins, which stabilize, bundle, or cross-link actin filaments and thus mediate the highly ordered microfilament organization essential for regulated growth, adhesion, and differentiation, have been classified as tumor suppressor proteins in a variety of experimental systems.

For profilins, which are believed to be primarily engaged in actin dynamics, tumor suppressor activity has not been described so far. It has been shown that overexpression of profilin in mammalian cell culture cells leads to a stabilization of actin filaments (29, 39), which may be directly caused by the actin polymerization-promoting activity of profilins. Furthermore, endothelial cells overexpressing profilin display increased adhesion to the substratum (28), another feature that has been correlated with a nonmalignant phenotype of cells. However, it is conceivable that the effects of an imbalance of actin-associated proteins on tumorigenicity are not directly linked to their mode of actin organization, but to their role in signal transduction to the actin cytoskeleton. In this context, it is noteworthy that gelsolin, another actin-binding protein involved in actin filament dynamics, has also been described as a tumor suppressor protein (40). Gelsolin and profilins both bind to the acidic phospholipid phosphatidylinositol 4,5-bisphosphate (PIP$_2$), a well-characterized mediator in several signal transduction pathways (31, 32), and are thus both considered important connectors at the cross-roads of PIP$_2$-dependent signal transduction (9, 41). For profilins, additional links to signal transduction pathways have to be considered. Several polyproline-rich proteins have now been identified as ligands for the poly-1-proline binding site on these small proteins in mammals. In this context, the vasodilator-stimulated phosphoprotein (VASP), which is a substrate for cAMP/cGMP-dependent kinases (16), and p140mDia, a formin-related protein comprising a rho-GTPase binding site in addition to a profilin-binding motif (15), should be mentioned. More recently, profilins have been identified as nuclear constituents and ligands for proteins involved in transcription and RNA processing (42). A low profilin 1 content, as indicated by our findings for the tumor cells described here, might therefore result in a cascade of consequences exceeding by far a simple reduction in profilin–actin complexes, leading to transformed properties and tumorigenicity.

References

1. Gioanni, J., D. Le Francoise, E. Zanghellini, C. Mazeau, F. Ettore, J.-C. Lambert, M. Schneider, and B. Dutrillaux. 1990. Establishment and characterization of a new tumorigenic cell line with a normal karyotype derived from a human breast adenocarcinoma. *Br. J. Cancer.* 62:8–13.
2. Theile, M., S. Hartmann, H. Scherthan, W. Arnold, W. Deppert, R. Frege, F. Glaab, W. Haensch, and S. Scherneck. 1995. Suppression of tumorigenicity of breast cancer cells by transfer of human chromosome 17 does not require tranferred BRCA1 and p53 genes. *Oncogene.* 10:439–447.
3. Wales, M.M., M.A. Biel, W. El Deiry, B.D. Nelkin, J.P. Issa, W.K. Cavenee, S.J. Kuerbitz, and S.B. Baylin. 1995. p53 activates expression of HIC-1, a new candidate tumor suppressor gene on 17p13.3. *Nat. Med.* 6:570–577.
4. Schultz, D.C., L. Vanderveer, D.B. Berman, T.C. Hamilton, A.J. Wong, and A.K. Godwin. 1996. Identification of two candidate tumor suppressor genes on chromosome 17p13.3. *Cancer Res.* 56:1997–2002.
5. Stack, M., D. Jones, G. White, D.S. Liscia, T. Venesio, G. Casey, D. Chrichton, S. Varley, E. Mitschell, S. Heighway, et al. 1995. Detailed mapping and loss of heterozygosity analysis suggests a suppressor locus involved in sporadic breast cancer within a distal region of chromosome band 17p13.3. *Hum. Mol. Genet.* 4:2047–2055.
6. Liang, P., and A.B. Pardee. 1992. Differential display of eukaryotic messenger RNA by means of the polymerase chain reaction. *Science.* 257:967–970.
7. Kwiatkowski, D.J., L. Aklog, D.H. Ledbetter, and C.C. Morton. 1990. Identification of the functional profilin gene, its localization to chromosome subband 17p13.3, and demonstration of its deletion in some patients with Miller-Dieker syndrome. *Am. J. Hum. Genet.* 46:559–567.
8. Theriot, J.A., and T.J. Mitchison. 1993. The three faces of profilin. *Cell.* 75:835–838.
9. Schlüter, K., B.M. Jockusch, and M. Rothkegel. 1997. Profilins as regulators of actin dynamics. *Biochim. Biophys. Acta.* 1359:97–109.
10. Carlsson, L., L.E. Nystrom, I. Sundkvist, F. Markey, and U. Lindberg. 1977. Actin polymerizability is influenced by profilin, a low molecular weight protein in non-muscle cells. *J. Mol. Biol.* 115:465–483.
11. Kang, F., D.L. Purich, and F.S. Southwick. 1999. Profilin promotes barbed-end actin filament assembly without lowering the critical concentration. *J. Biol. Chem.* 274:36963–36972.
12. Pantaloni, D., and M.F. Carlier. 1993. How profilin promotes actin filament assembly in the presence of thymosin beta 4. *Cell.* 75:1007–1014.
13. Goldschmidt-Clermont, P.J., L.M. Machesky, J.J. Baldassare, and T.D. Pollard. 1990. The actin-binding protein profilin binds to PIP2 and inhibits its hydrolysis by phospholipase C. *Science.* 247:1575–1578.
14. Lu, P.J., W.R. Shieh, S.G. Rhee, H.L. Yin, and C.S. Chen. 1996. Lipid products of phosphoinositide 3-kinase bind human profilin with high affinity. *Biochemistry.* 35:14027–14034.
15. Watanabe, N., P. Madaule, T. Reid, T. Ishizaki, G. Watanabe, A. Kakizuka, Y. Saito, K. Nakao, B.M. Jockusch, and S. Narumiya. 1997. p140mDia, a mammalian homolog of *Drosophila diaphanous*, is a target protein for Rho small GTPase and is a ligand for profilin. *EMBO (Eur. Mol. Biol. Organ.) J.* 16:3044–3056.
16. Reinhard, M., K. Giehl, K. Abel, C. Haffner, T. Jarchau, V. Hoppe, B.M. Jockusch, and U. Walter. 1995. The proline-rich focal adhesion and microfilament protein VASP is a ligand for profilins. *EMBO (Eur. Mol. Biol. Organ.) J.* 14:1583–1589.
17. Koi, M., M. Shimizu, H. Morita, H. Yamada, and M. Oshimura. 1989. Construction of mouse A9 clones containing a single human chromosome tagged with neomycin-resistance gene via microcell fusion. *Jpn. J. Cancer Res.* 8:413–418.
18. Chomzynski, P., and N. Sacchi. 1987. Single-step method of RNA isolation by acid guanidinium thiocyanate-phenol-chloroform extraction. *Anal. Biochem.* 162:156–159.
19. Kroczek, R.A. 1993. Southern and northern analysis. *J. Chromatogr.* 618:133–145.
20. Yoo, H.W., C.A. Warner, C.H. Chen, and R.J. Desnick. 1993. Hydroxymethylbilane synthase: complete genomic sequence and amplifiable polymorphisms in the human gene. *Genomics.* 15:21–29.
21. Bieche, I., I. Laurendeau, S. Tozlu, M. Olivi, D. Vidaud, R. Lidereau, and M. Vidaud. 1999. Quantitation of MYC gene expression in sporadic breast tumors with a real-time reverse transcription-PCR assay. *Cancer Res.* 59:2759–2765.
22. Sealey, L., and R. Chalkley. 1987. At least two nuclear proteins bind specifically to the Rous sarcoma virus long terminal repeat enhancer. *Mol. Cell. Biol.* 7:787–798.
23. Mayboroda, O., K. Schlüter, and B.M. Jockusch. 1997. Differential colocalization of profilin with microfilaments in PtK2 cells. *Cell Motil. Cytoskeleton.* 37:166–177.
24. Theile, M., S. Hartmann, H. Naundorf, D. Ruess, B. Elbe, H. Krause, W. Deppert, J.C. Barrett, and S. Scherneck. 1994. Wild-type p53 is not involved in reversion of the tumorigenic phenotype of breast cancer cells after transfer of normal chromosome 17. *Int. J. Oncol.* 4:1067–1075.
25. Kölble, K., O.M. Ullrich, H. Pidde, B. Barthel, J. Diermann, B. Rudolph, M. Dietel, P.M. Schlag, and S. Scherneck. 1999. Microsatellite alterations in serum DNA of patients with colorectal cancer. *Lab. Invest.* 79:1145–1150.
26. Hamburger, A.W., and S.E. Salmon. 1977. Primary bioassay of human tumor stem cells. *Science.* 197:461–463.
27. Petersen, O.W., L. Ronnov-Jessen, A.R. Howlett, and M.J. Bissell. 1992. Interaction with basement membrane serves to rapidly distinguish growth and differentiation pattern of normal and malignant human breast epithelial cells. *Proc. Natl. Acad. Sci. USA.* 89:9064–9068.
28. Moldovan, N.I., E.E. Milliken, K. Irani, J. Chan, R.H. Sohn, T. Finkel, and P.J. Goldschmidt-Clermont. 1997. Regulation of endothelial cell adhesion by profilin. *Curr. Biol.* 7:24–30.
29. Rothkegel, M., O.A. Mayboroda, M. Rohde, C. Wucherpfennig, R. Valenta, and B.M. Jockusch. 1996. Plant and animal profilins are functionally equivalent and stabilize microfilaments in living animal cells. *J. Cell Sci.* 109:83–90.
30. Baatout, S. 1996. Profilin: an update. *Eur. J. Clin. Chem.*

Clin. Biochem. 34:575–577.

31. Puius, Y.A., N.M. Mahoney, and S.C. Almo. 1998. The modular structure of actin-regulatory proteins. *Curr. Opin. Cell Biol.* 10:23–34.

32. Ayscough, K.R. 1998. In vivo functions of actin-binding proteins. *Curr. Opin. Cell Biol.* 10:102–111.

33. Ben Ze'ev, A. 1997. Cytoskeletal and adhesion proteins as tumor suppressors. *Curr. Opin. Cell Biol.* 9:99–108.

34. Button, E., C. Shapland, and D. Lawson. 1995. Actin, its associated proteins and metastasis. *Cell Motil. Cytoskeleton.* 30: 247–251.

35. Braverman, R.H., H.L. Cooper, H.S. Lee, and G.L. Prasad. 1996. Anti-oncogenic effects of tropomyosin: isoform specificity and importance of protein coding sequences. *Oncogene.* 13:537–545.

36. Glück, U., D.J. Kwiatkowski, and A. Ben Ze'ev. 1993. Suppression of tumorigenicity in simian virus 40-transformed 3T3 cells transfected with alpha-actinin cDNA. *Proc. Natl. Acad. Sci. USA.* 90:383–387.

37. Rodriguez Fernández, J.L.R., B. Geiger, D. Salomon, I. Sabanay, M. Zöller, and A. Ben-Ze'ev. 1992. Suppression of tumorigenicity in transformed cells after transfection with vinculin cDNA. *J. Cell Biol.* 119:427–438.

38. Jockusch, B.M., and M. Rüdiger. 1996. Crosstalk between cell adhesion molecules: vinculin as a paradigm for regulation by conformation. *Trends Cell Biol.* 6:311–315.

39. Finkel, T., J.A. Theriot, K.R. Dise, G.F. Tomaselli, and P.J. Goldschmidt-Clermont. 1994. Dynamic actin structures stabilized by profilin. *Proc. Natl. Acad. Sci. USA.* 91:1510–1514.

40. Asch, H.L., K. Head, Y. Dong, F. Natoli, J.S. Winston, J.L. Connoly, and B.B. Asch. 1996. Widespread loss of gelsolin in breast cancers of humans, mice, and rats. *Cancer Res.* 56: 4841–4845.

41. Yin, H.L. 1987. Gelsolin: calcium- and polyphosphoinositide-regulated actin-modulating protein. *Bioessays.* 7:176–179.

42. Giesemann, T., S. Rathke-Hartlieb, M. Rothkegel, J. Bartsch, S. Buchmeier, B.M. Jockusch, and H. Jockusch. 1999. A role for polyproline motifs in the spinal muscular atrophy protein SMN. Profilins bind to and colocalize with *smn* in nuclear gems. *J. Biol. Chem.* 274:37908–37914.